Ceramics-Silikáty 65 (1), 83-89 (2021)
www.ceramics-silikaty.cz doi: 10.13168/cs.2021.0005

EFFECT OF TITANIUM PARTICLES ON THE MICROSTRUCTURE AND MECHANICAL PROPERTIES OF ALUMINA MATRIX COMPOSITES

#JOSÉ RODRÍGUEZ-GARCÍA*, ENRIQUE ROCHA-RANGEL*, CARLOS CALLES-ARRIAGA*, ELIZABETH REFUGIO-GARCÍA**, RICARDO LÓPEZ-GARCÍA***, ARACELI MALDONADO REYES***

*Universidad Politécnica de Victoria, Av. Nuevas Tecnologías 5902, Parque Científico y Tecnológico de Tamaulipas, Ciudad Victoria, Tamaulipas, México, 87138
**Universidad Autónoma Metropolitana, Av. San Pablo 180, Col. Reynosa Tamaulipas, CDMX, México, 02200
***Tecnológico Nacional de México/Instituto Tecnológico de Ciudad Victoria, Blvd. Emilio Portes Gil No. 1301 Pte. Cd. Victoria Tamps., México, 87010

#E-mail: jrodriguezg@upv.edu.mx

Submitted November 18, 2020; accepted January 14, 2021

Keywords: Composites, Mechanical properties, Microstructure, Structural characterization

In this study, Al_2O_3-based composites strengthened with Ti were manufactured. High-energy milling was used to mix and grind the raw materials (450 rpm during 40 min). These powders were compacted (300 MPa) into cylindrical samples and sintered at 1500 °C for 2 h. Scanning electron microscopy observations show dense, fine and homogeneous microstructures, with a uniform distribution of metal particles throughout the ceramic matrix. A significant effect on the composite micro-hardness can be observed (as the titanium percentage is increased, micro-hardness is also increased). In other words, composites have a significant surface hardness, which diminishes towards the center of the piece. This attribute is highly useful for solid elements exposed to extreme strain and shearing conditions since hardness allows withstanding wear, corrosion, and friction, but the soft center allows withstanding vertical loads in the piece cross section. The fracture toughness, estimated by the indentation fracture method, showed that the manufactured composites here present higher values up to 100 % than the control sample's average (0.0 % Ti). Hence, it can be inferred that titanium particles in a ceramic matrix can disperse the energy of cracks spreading.

INTRODUCTION

New materials are being developed every day to provide specific technological solutions; these materials are called advanced materials or structural materials. These materials are prepared according to industry needs, e.g., electric, electronic, optical, mechanical, biomedical, aeronautic, and civil engineering systems, among others. Advanced materials require intense research and the development of sophisticated characterization methods, mainly at microscopic levels. Hence, it is necessary to develop of procedures to alter or modify its properties in order to produce improved materials and therefore, new applications [1-4].

Advanced ceramics are a great option because of their physical-chemical properties (high hardness and resistance to compression, high corrosion resistance, high melting point, excellent chemical and structural stability at high temperatures, and high elastic modulus). However, their applications as structural materials are somewhat limited because of their brittleness, i.e., too low fracture toughness. For example, alumina (Al_2O_3) ceramic has a wide range of applications nowadays: its high hardness (9 on the Mohs scale) make it useful in cutting tools, while its high melting point (until 2000 °C) and chemical stability make it suitable as a refractory material, including high-temperature insulation. Moreover, it is an electric insulation material, and it is inert and insoluble to almost all chemical reagents. It is also biocompatible, allowing it to be adopted by the human body (joints, bones, dental implants and hearing aids). However, as a particular characteristic of all ceramics, it has low fracture toughness (i.e., low resistance to crack propagation) and high brittleness (i.e., low resistance to tension, flexion, or perpendicular loads) [5, 6].

Ceramic-matrix composites (CMCs) based on a ceramic matrix reinforced with metallic particles (also called cermets) allow combining ceramics and metals' properties. However, a critical issue is a difference in deformation mechanism and thermal expansion coefficients during sintering. Alumina-matrix composites reinforced with metal and intermetallic particles are examples of CMCs (cermets) [7-11].

Yaoa *et al*. [12] applied plasma spark sintering for to prepare alumina-based composite reinforced with nickel particles, reporting a fracture toughness of 3.84 $MPa \cdot m^{-0.5}$. In another study, Sekino *et al*. [13] synthesized the same type of composite developed by hydrogen reduction of NiO to Ni and subsequent hot-pressing of alumina with nickel oxide mixture, reporting a maximum fracture toughness of 3.5 $MPa \cdot m^{-0.5}$ with 5 % in nickel volume. Ji and Yeomans [14] synthesized

alumina-based composites reinforced with chromium particles through hot pressing with temperatures of 1400 °C and 1600 °C, reporting fracture toughness values of 4.7 MPa·m$^{-0.5}$, concluding that a relatively high content of chromium is necessary to improve this property. Following the same approach, Guichard *et al.* [15] synthesized alumina-based composites reinforced with 22 vol. % of chromium particles, reporting a crack stress intensity factor of 7.2 MPa·m$^{-0.5}$. Prielipp *et al.* [16] synthesized alumina-based composites reinforced with aluminum metal particles, indicating a crack toughness of 10.5 MPa·m$^{-0.5}$ with 35 % of aluminum. Recently, alumina-based composites reinforced with titanium particles have been developed under different conditions, reporting favorable densification results, micro-hardness, and fracture toughness [17-22].

In general, it is observed that the reinforcement size and its homogeneous distribution in the ceramic matrix contributes to obtaining the best mechanical properties, mainly the critical stress intensity factor (fracture toughness). Therefore, this work aims at preparing alumina-based composites reinforced with titanium nanoparticles by powder, using small amounts of reinforcing material with high speed and short milling time. The primary purpose of this paper is to study the effect of the grinding conditions on the mechanical properties (hardness and fracture toughness) in the cross section of the samples.

EXPERIMENTAL

Al_2O_3 powder (Sigma-Aldrich, purity 99.9 %, size 5 μm) and Ti powder (Mayer, purity 99.9 %, size 5 μm) were used to synthesize the samples. Four systems were studied, all with alumina as the ceramic matrix. The content of the reinforcing metal (Ti) that was used was 0.2, 0.4, 0.5 and 1.0 wt. %. In addition, a sample without reinforcing material was prepared (control sample) in order to have reference values. The grinding and mixing of the powders were performed by high energy milling using a planetary mill (Retsch, PM100, Germany) in a stainless steel container with a volume of 250 ml and ZrO_2 grinding media (balls) of 3 mm diameter. The ratio between powder weight/ball weights was 1:14, using an overall volume of 1/3 of the container. Speeds of 450 rpm were used for 40 minutes in dry with cycles of 3 minutes for each direction for rotation and pauses of 10 seconds between cycles. The powders' particle size distribution resulting from the grinding was determined using laser diffraction (Malvern Masterziser 2000, UK). Cylindrical samples of each composition with 20 mm of diameter and 3 mm thickness were manufactured by uniaxial pressing, using 350 MPa pressure (Montequipo 20 t hydraulic press, Mexico). The green samples were sintered in an electric furnace (Thermo Scientific Lindberg Blue, Germany) at 1500 °C for 2 hours with a heating rate of 5 °C·min^{-1} and an argon flow of gas of 10 cm^3·min^{-1} in the furnace chamber. The dwell time at maximum temperature was 120 minutes.

The Archimedes method was used to measure the density of the sintered samples. For this purpose, each study system's density was calculated using the mixing rule, using density values of 3.96 g·cm^{-3} and 4.54 g·cm^{-3} for alumina and titanium, respectively. An optical microscope (Nikon, MA200, Japan) and a scanning electron microscope (JEOL 6300, Japan) were employed to observe milled powders and microstructures of sintered samples. The micro-hardness and fracture toughness were estimated by the indentation fracture method, using a Vickers micro-hardness tester (Wilson Instruments, S400, Japan) with a pyramidal diamond tip indenter using a force of 9.8 N with a penetration time of 10 s and applying the Evans and Charles Equation [23].

RESULTS

Particle size distribution

The cumulative distribution for the samples milled at 450 rpm for 40 min and different titanium contents is reported in Figure 1. Generally speaking, there is no significant effect of Ti content on the accumulated distribution of particles, especially in sizes smaller than 6 microns, since the volume of this distribution is very similar in all cases.

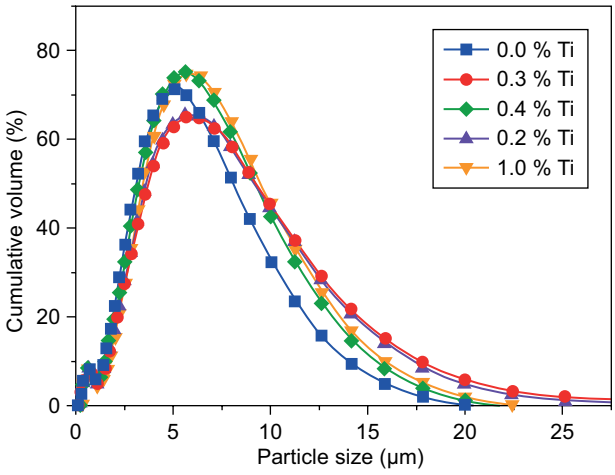

Figure 1. Particle size distributions after milling (450 rpm for 40 min).

For a better interpretation of this figure, deciles D10, D50 (median), and D90 were taken, from here we have that the accumulated distribution of particle size in the first decile (D10) is approximately 1.5 microns; for the median (D50), we have an accumulated distribution of 3 microns in the particle size and for the decile D90 the accumulated distribution of particle size is 18 microns. Of these results, 50 % of the accumulated volume of

particles' distribution has very fine sizes and less than 3 microns, which should be suitable for the sintering stage because there is a smaller separation distance between particles, which favors the atomic diffusion process during sintering. Consequently, well-densified bodies with a more homogeneous microstructure can be obtained, which should be favorable for mechanical properties.

Density

The results of the relative density measurements of sintered samples are shown in Figure 2. A high percentage of density is observed in all samples, including the control sample (without titanium particle inclusions); it can be noticed that the relative density is directly proportional to the titanium particles content. The overall high relative density is partly due to the appropriate distribution of particle sizes in the powders that favored a larger number of contacts between them and improved diffusion during sintering. On the other hand, the improvements in densification with titanium increments can be explained by the fact that titanium as a metal is a good heat conductor, which favors both heat and mass transfer phenomena during sintering.

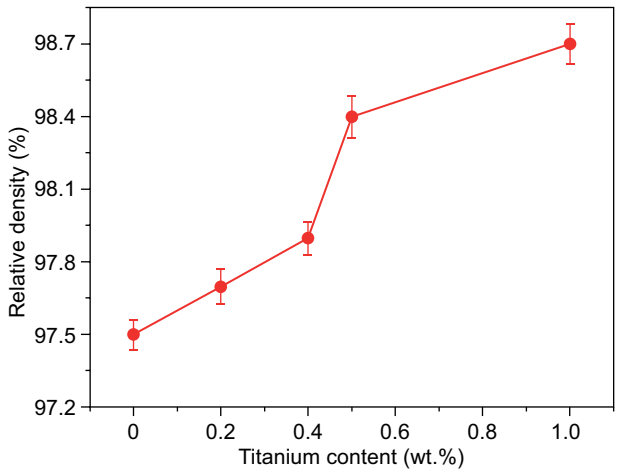

Figure 2. Relative density of the sintered samples as a function of titanium content.

Microstructure

Figure 3 shows micrographs obtained by Scanning Electron Microscopy (SEM) of thermally treated samples with 0.5 % and 1 % of titanium. Figures 3a and 3b were taken at the same magnification (1000 ×). There are significant differences regarding the grain size and the matrix solidification process. With respect to the sample with 0.5 % of titanium (Figure 3a) the grains present sizes between 5 and 10 μm. In the sample with 1 % of titanium (Figure 3b), there are hemispherical particles with sizes from 1 to 4 μm and acicular particles with sizes from 5 to 10 μm. Concerning the metallic aggregates, the same particle size (approximately 1μm) is observed in both cases, with a uniform distribution throughout the sample and agglomerates in some areas. Figure 3c is a close up (5000 ×) zoom into a selected zone from Figure 3b to visualize the matrix and titanium particles. The chemical elements present in our samples are visible on the EDS spectrum in Fig. 3c. As expected, it can be observed that

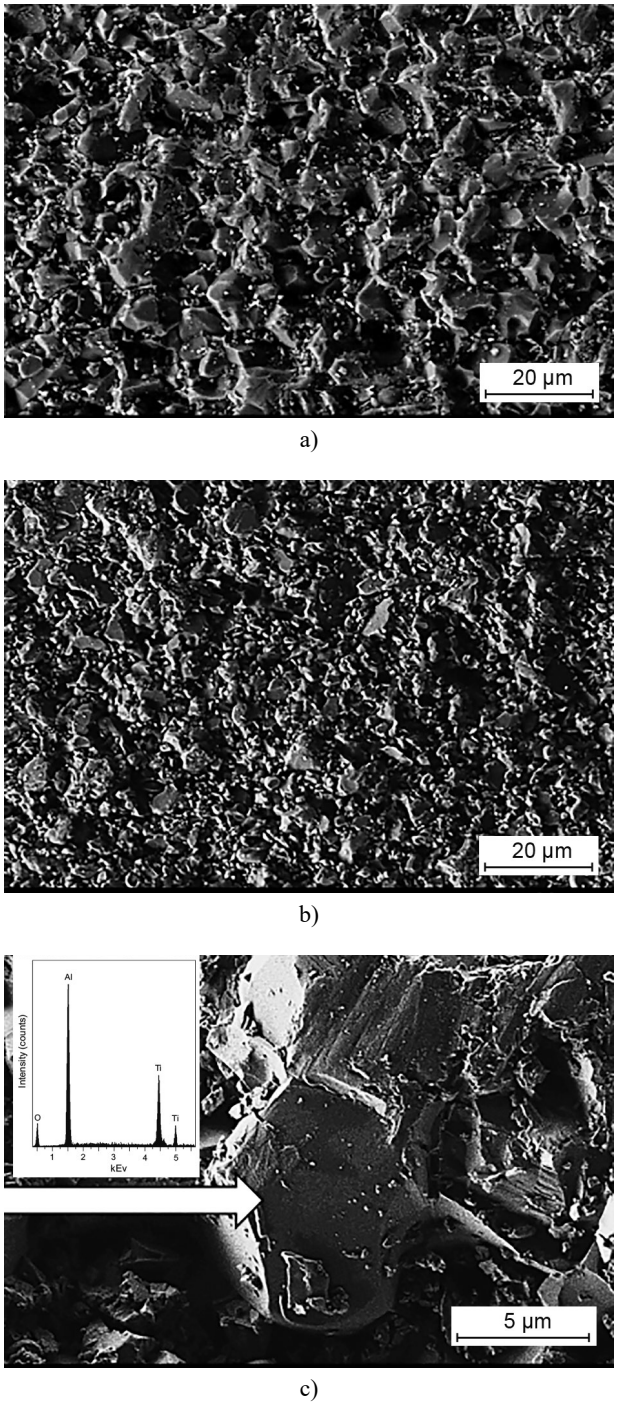

Figure 3. SEM micrographs of sintered samples: a) alumina matrix with 0.5 %Ti, b) alumina matrix with 1.0 % Ti, c) zoom of image (b).

the matrix is formed by alumina particles, Al and O (gray zone), and the inclusions are the metallic reinforcement, Ti (small white particles), see Figure 3c. In Figures 3c, b, the EDS analysis was essentially the same everywhere, indicating a homogeneous distribution of the metallic particles (small white particles) in the ceramic matrix (gray particles). Both samples (with 0.5 and 1 % of titanium) showed an efficient densification process. In this process, titanium particles behave as efficient heat transfer media during thermal treatment by their metallic nature. Thus, the atomic diffusion process is facilitated, and consequently, better densification (and possibly a higher grain growth rate) are achieved.

Figure 4 shows an elemental mapping of samples sintered at 1500 °C. Figure 4a shows a homogeneous distribution of the elements present in the composite, aluminum (yellow dots) and oxygen (green dots), as well as the uniform distribution of titanium particles throughout the matrix (white dots).

On the other hand, Figure 4b shows that the ceramic matrix elements do not cover the entire sample uniformly; thus, there is a lack of these elements in some zones. There are a higher amount of distributed particles in the ceramic matrix for titanium, but in contrast to the previous sample, the inclusions are more agglomerated. This may imply that the sample is affected by agglomeration due to saturation, and likewise, the excess of titanium may generate a non-uniform densification matrix.

Micro-hardness

Figure 5 shows the average of the micro-hardness results from 14 measurements carried out on the studied samples' surface. It can be observed that the amount of metal reinforcements has a significant effect on the micro-hardness of the composite. Hence, for the control sample (0.0 % Ti), a micro-hardness of 630 HV was registered. As the titanium percentage is increased, there is a micro-hardness increase, reaching results of 1564 HV and 1593 HV for samples with 0.5 % Ti and 1 % Ti, respectively. The obtained results exceed the control sample values (1500HV). The sintering time affects the microstructure and its densification. As mentioned before, reinforcement effects in ceramic matrix regarding micro-hardness may be supported by an appropriate particle size distribution in the powders that favors a greater number of contacts between the particles and thus improved diffusion during sintering. On the other hand, titanium is a better heat conductor than alumina, which causes an acceleration in the diffusion of atoms. Hence, the mechanical properties of the composites are improved in comparison with the control sample.

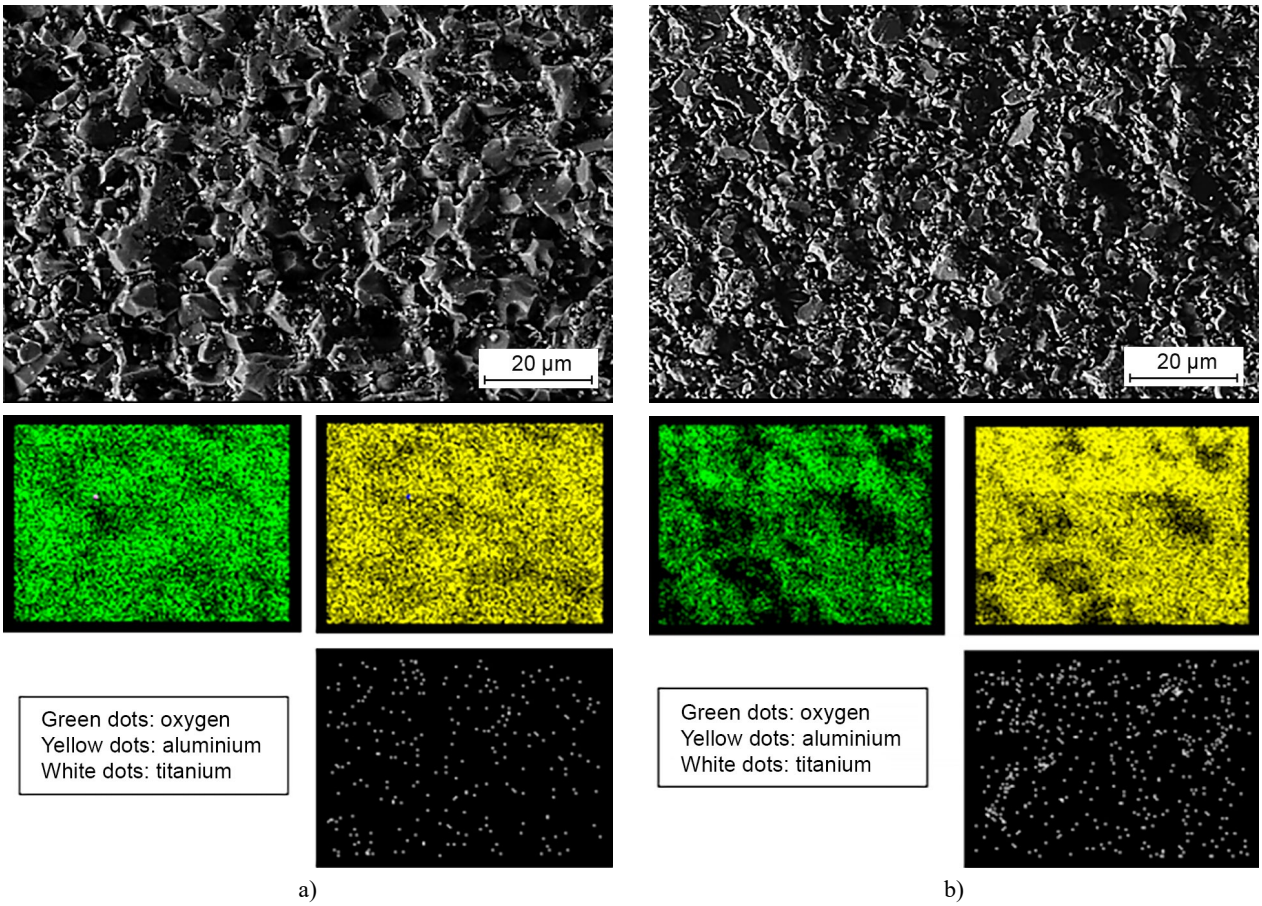

Figure 4. Elemental EDS mapping of thermally treated samples: a) alumina matrix with 0.5 % Ti, alumina matrix with 1.0 % Ti.

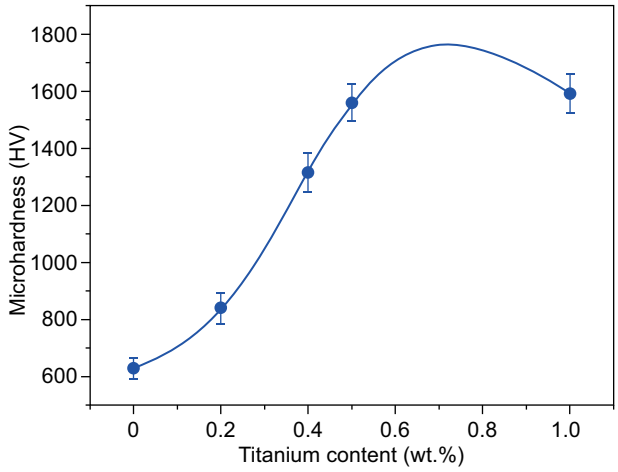

Figure 5. Micro-hardness at the surface of the samples as a function of titanium content.

In order to complement the results, samples with 0.5 % and 1 % of titanium were transversally sectioned to make a sweep of the local internal micro-hardness. Four domain zones were determined where micro-hardness tests of approximately 50 µm for each domain were carried out. The first domain (X_1) was located in the sample center, approximately 1500 µm from the surface. The second and third domain (X_2 y X_3) were located at 1000 µm and 500 µm from the surface, respectively. Finally, the fourth domain (X_4) was located closest to the surface (considering an extension of 50 µm for the domain itself). Results are shown in Figure 6.

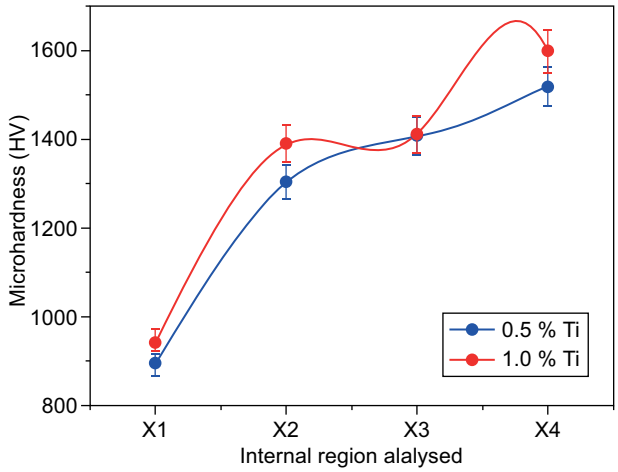

Figure 6. Local internal micro-hardness obtained on transverse cross sections of the samples.

In both cases, 0.5 and 1.0 % Ti, in the first domain circle X_1, micro-hardness values of 900 and 950 HV are reported respectively. In the second domain circle X_2, micro-hardness was increased from 1300 HV for the sample with 0.5 % Ti and 1400 HV in the sample with 1.0 % Ti. In the third domain circle, X_3, a micro-hardness of 1400 HV was reported for both samples. Regarding the fourth domain, X_4, a significant difference in reported results was observed. For the sample with 0.5 % Ti, a 1500 HV hardness was measured. In contrast, the sample with 1.0 % Ti exhibited a hardness of more than 1600 HV, possibly due to slight oxidation of the titanium on the composite's surface. According to the results, the composites have a significant surface hardness, which diminishes towards the center of the piece, thus maintaining fracture toughness. This feature of the composites is highly useful for solid elements that will be exposed to extreme conditions of strain and shearing since the hard surface allows withstanding wear, corrosion, and friction, among others, but the soft center allows withstanding vertical loads in the piece cross-section and increases the fracture resistance of the part.

Fracture toughness

Figure 7 shows an average fracture toughness results from 14 measurements carried out on the sample surface. It is noticed that the sample without titanium has a value below 4 MPa·m$^{-0.5}$, i.e., below the value of the control sample. A significant increase in fracture toughness is observed as the amount of titanium increases. The best results were found in samples with 0.5 % and 1.0 % of titanium particles. Still, already for 0.2 % and 0.4 % of titanium particles there is an increase in fracture toughness by about 25 % compared to the control sample. In the sample reinforced with 0.5 % of titanium, fracture toughness of 7.4 MPa·m$^{-0.5}$, approximately 90 % of the control sample value, was achieved. Still, can be surmised that the steep increase between 0.4 and 0.5 % of titanium is just due to a statistical sample-to-sample variation (that means, compared to a representative batch of samples, either the 0.4 % value is slightly to low or the 0.5 % value is slightly to high).

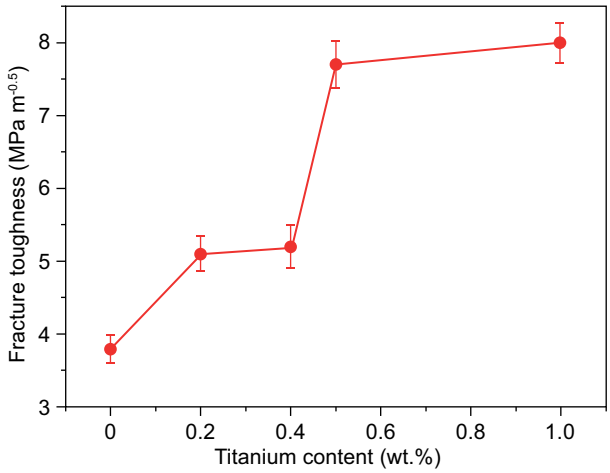

Figure 7 Fracture toughness obtained from indentations at the surface of the samples as a function of titanium content.

The highest fracture toughness value registered, approximately 8 MPa·m$^{-0.5}$ (which is more than twice the value of the control sample), was obtained for the sample reinforced with 1 % of titanium. It can be concluded that titanium increases not only the relative density and hardness but also the fracture toughness of the sintered samples. These increments can naturally be explained by ductile metallic inclusions, which increase the fracture toughness of the composite compared to the brittle alumina ceramics (matrix material). When a crack is generated and impinges on an inclusion, the ductile deformation of the elastoplastic inclusion consumes energy that is not available anymore for crack propagation.

Figure 8 shows local internal fracture toughness (average results obtained from 14 measurements) of the composite samples with 0.5 and 1 % of titanium particles. These local results are from the sample's inner parts (i.e., the same as considered above in the measurement of local internal micro-hardness) with locations denoted as X_1, X_2, X_3, X_4 (see the detailed explanation above). In the case of the first location (X_1), values of 4.3 MPa·m$^{-0.5}$ and 5 MPa·m$^{-0.5}$ were obtained for samples A and B, respectively (A: 0.5 % Ti and B: 1 % Ti). Values for samples with 0.5 % Ti are slightly lower than those for the control sample, while samples with 1.0 % Ti are above the reference value. In the second location (X_2), similar values were registered for both samples (6.3 MPa·m$^{-0.5}$ for samples with 0.5 % Ti and 6.5 MPa·m$^{-0.5}$ for samples with 1.0 % Ti). These values correspond to approximately 45 % increase with respect to the control sample. A similar situation was observed at the third location (X_3), with 6.9 MPa·m$^{-0.5}$ for samples with 0.5 % Ti and 7 MPa·m$^{-0.5}$ for samples with 1.0 % Ti, i.e., values corresponding to a 65 % increase with respect to the control sample. In the last location close to the surface (X_4), values of 8 MPa·m$^{-0.5}$ were obtained for samples with 0.5 % Ti and 8.1 MPa·m$^{-0.5}$ for samples with 1.0 % Ti (87 % increase compared to the control sample). It can be concluded that there is a progressive fracture toughness increase from the center to the surface of the sample, similar in slope to the micro-hardness results.

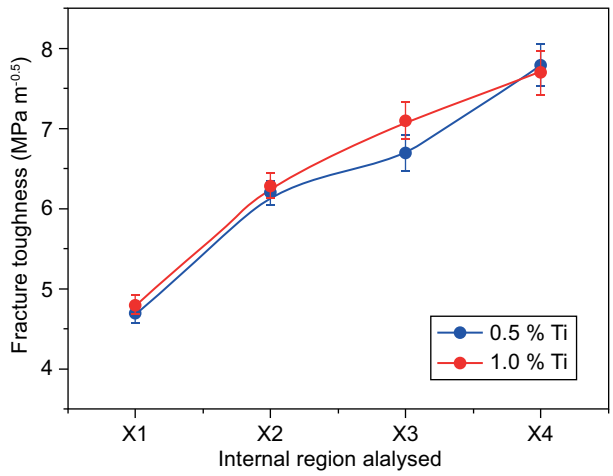

Figure 8 Local internal fracture toughness obtained on transverse cross sections of the samples.

CONCLUSIONS

In this work, dense alumina-matrix composites with titanium nanoparticles (homogeneously distributed in the ceramic matrix) were prepared and characterized. The grinding conditions used in this work were effective, resulting in an appropriate particle size, where 50 % of the accumulated volume of the distribution of particles has very fine sizes and less than 3 microns, which should be suitable for the sintering stage because there is a smaller separation distance between particles, which favors the atomic diffusion process during sintering, which was obviously favorable for the densification for the composite samples. With increased speed of rotation and reduced grinding time, composites were obtained with mechanical properties similar to those reported in the literature. The difference was the much lower energy consumption (in this work, 60 % of electricity was saved in the grinding stage). The best results in terms of hardness and fracture toughness were those obtained in the samples with 0.5 % and 1.0 % of titanium, with a micro-hardness of approximately 1600 HV and a fracture toughness of approximately 8 MPa·m$^{-0.5}$. The titanium particles in the ceramic matrix can disperse the energy of cracks spreading. The mechanical properties mentioned above decrease below 0.5 % of titanium particles. Moreover, the cross section's local analyses reveal a decrease in hardness and toughness when approaching the center of the samples. These results mean that the composites are tenacious (hard surface outside and soft core inside), which may open the way to interesting applications of these materials.

REFERENCES

1. Wessel J. K. (2004). *The Handbook of Advanced Materials: Enabling New Designs.* 1st ed. Wiley John Wiley & Sons Inc.
2. Miyamoto Y., Kaysser W.A., Rabin B.H., Kawasaki A., Ford R.G. (1999). *Functionally Graded Materials: Design, Processing and Applications.* 1st ed. Springer Science Business Media, LLC.
3. Ctibor P., Kraus L., Tuominen J., Vuoristo P., Chraska P. (2007). Improvement of mechanical properties of alumina and zirconia plasma sprayed coatings induced by laser post-treatment. *Ceramics-Silikáty*, *51*(4), 181-189.
4. Guo J., Zhou H., Fan T., Zhao B., Shang X., Zhou T., He Y. (2020). Improving electrical properties and toughening of PZT-based piezoelectric ceramics for high-power applications via doping rare-earth oxides. *Journal of Materials Research and Technology, 9*(6), 14254-14266. doi: 10.1016/j.jmrt.2020.10.022

5. Barsoum M.W. (2019). *Fundamentals of Ceramics.* 2nd ed. Taylor and Francis.
6. Okayasu M., Sugiyama E., Mizuno M. (2010). In situ measurement of material properties of lead zirconate titanate piezoelectric ceramics during cyclic mechanical loading. *Journal of the European Ceramics Society, 30*(6), 1445-1452. doi: 10.1016/j.jeurceramsoc.2009.11.004.
7. Szafran M., Konopka K., Bobryk E., Kurzydłowski K.J. (2007). Ceramic matrix composites with gradient concentration of metal particles. *Journal of the European Ceramic Society, 27*(2-3), 651–654. doi: 10.1016/j.jeurceramsoc.2006.04.046.
8. Daguano J., Santos C., Souza R.C., Balestra R.M., Strecker K., Elias C.N. (2007). Properties of ZrO_2-Al_2O_3 composite as a function of isothermal holding time. *International Journal of Refractory Metals and Hard Materials, 25*(5), 374–379. doi: 10.1016/j.ijrmhm.2006.12.005.
9. Liu C., Zhang J., Sun J., Zhang X. (2007). Addition of Al–Ti–B master alloys to improve the performances of alumina matrix ceramic materials. *Ceramics International, 33*(7), 1319-1324. doi: 10.1016/j.ceramint.2006.04.014.
10. Marcin C., Katarzyna P. (2007). Processing, microstructure and mechanical properties of Al_2O_3-Cr nanocomposites. *Journal of the European Ceramic Society, 27*(2-3), 1273-1279. doi: 10.1016/j.jeurceramsoc.2006.05.093.
11. Stratigaki M., Pabst W., Nečina V., Hajíček M., Gotsis A. D. (2019): Microstructure and mechanical properties study of slip-cast copper-alumina composites, *SN Appl. Sci. 1* (1), paper No. 40. Doi:10.1007/s42452-018-0037-4.
12. Yao X., Huang Z., Chen L., Jiang D., Tan S., Michel D., Wang G., Mazerolles L., Pastol J. (2005): Alumina-nickel composites densified by spark plasma sintering. *Materials Letters, 59*(18), 2314–2318. doi: 10.1016/j.matlet.2005.03.012.
13. Sekino T., Nakajima T., Niihara K. (1996): Mechanical and magnetic properties of nickel dispersed alumina-based nanocomposite. *Materials Letters, 29*(1-3), 165–169. doi: 10.1016/S0167-577X(96)00136-X.
14. Ji Y., Yeomans J.A. (2002): Processing and mechanical properties of Al_2O_3-5 vol.% Cr nanocomposites. *Journal of the European Ceramic Society, 22*(12), 1927-1936. doi: 10.1016/S0955-2219(01)00528-3.
15. Guichard J.L., Tillement O., Mocellin A. (1998): Alumina-Chromium cermets by hot-pressing of nanocomposite powders. *Journal of the European Ceramic Society, 18*(12), 1743-1752. doi: 10.1016/S0955-2219(98)00009-0.
16. Prielipp H., Knechtel M., Claussen N., Streiffer S.K., Müllejans H., Rühle M., Rödel J. (1995): Strength and fracture toughness of aluminum/alumina composites with interpenetrating networks. *Materials Science and Engineering: A, 197*(1), 19-30. doi: 10.1016/0921-5093(94)09771-2.
17. Travitzky N., Gotman I., Claussen N. (2003): Alumina-Ti aluminide interpenetrating composites: microstructure and mechanical properties. *Materials Letters, 57*(22-23), 3422-3426. doi: 10.1016/S0167-577X(03)00090-9.
18. Rocha E., Hernández D., Torrés E., Martínez E., Díaz S. (2010): Alumina-based composites strengthened with titanium and titanium carbide dispersion. *Materials Technology, 62*(3), 75-78. doi: 10.14382/epitoanyag-jsbcm.2010.15.
19. Rocha E., Rodríguez J., Refugio E., Hernández D., Terrés E. (2014): Microstructure of alumina-matrix functional graded materials reinforced with nanometric titanium and TiO_2, TiC or TiN dispersions. *Journal Pensee*, 76(4), 296–301.
20. Rocha E., Rodríguez J., Esparza S., Cruz B., Estrada I., Martínez R. (2016): Effect of particle size and titanium content on the fracture toughness of particle-ceramic composites. *Materials Today: Proceedings, 3*(2), 249–257. doi: 10.1016/j.matpr.2016.01.066.
21. Esparza S., Rocha E., Rodríguez J., Hernández C. (2013): Strengthening of alumina-based ceramics with titanium nanoparticles. *Materials Science and Applications, 5*(7), 467-474. doi: 10.4236/msa.2014.57050.
22. Refugio E., Hernández D., Torrés E., Rodríguez J., Rocha E. (2012): Microstructure of alumina-matrix composites reinforced with nanometric titanium and titanium carbide dispersions. *Materials Research, 15*(6), 898-902. doi: 10.1590/S1516-14392012005000110.
23. Evans A.G., Charles E.A. (1976): Fracture toughness determinations by indentation. *Journal of the American Ceramic Society*, *59*(7-8), 371-372. doi: 10.1111/j.1151-2916.1976.tb10991.x.